JOURNAL OF MATERIALS SCIENCE 14 (1979) 920–930

Size effect on the strength of glassy carbon

R. E. BULLOCK, J. L. KAAE
General Atomic Company, San Diego, California, USA

Three-point bend tests were conducted on three sets of commercial glassy carbon specimens having volumes of V, $2V$, and $4V$, and mean strengths of these specimens decreased with increasing volume (from 37 to 32 to 28 $\times$ 10^3 psi). These results are in good agreement with Weibull predictions of $\sigma(V) = 1.12\sigma(2V) = 1.26\sigma(4V)$, which are based on a uniform distribution of flaws throughout a volume of material that is characterized by a Weibull modulus of $m = 6.0$. Moreover, the resulting strength formulation for any volume $V(\text{in.}^3)$, $\sigma = 6\,V^{-1/6} \times 10^3$ psi, correlates well with wider-spread data from other sources. In common with other brittle materials, glassy carbon satisfies the crack bifurcation relationship of $\sigma r^{1/2}$ = constant, and this was used to provide additional support for the validity of the volume-dependent Weibull theory. Failures in this material usually originated at interior spherical pores, and the mean size of these flaws for different sets of specimens increased with test volume.

1. Introduction

Weibull theory accounts reasonably well for differences found in the mean strength of a brittle material when specimens of roughly the same size are tested by various methods that produce different stress distributions [1–10], but predictions are not usually as good when sets of specimens of widely differing sizes are tested by the same method [8–18]. However, there are at least two sources of error that apparently have not been simultaneously eliminated in most of the studies on size effects, namely: (1) the change in strain-rate with size has not usually been considered [19], and this effect can be large for those non-carbonaceous ceramics that are more subject to static fatigue [20–21], and (2) specimen sizes for most graphites and other large-grained ceramics have often not been large enough to adequately represent polycrystalline behaviour [22].

Strain-rate effects tend to cancel Weibull statistical effects on measured strengths for the cases most often studied in which specimens of different thicknesses have been tested over the same span length [19], and it is noteworthy that such experimental size effects are usually considerably less than Weibull predictions based on statistical effects alone [8–16]. Fewer studies have been conducted in which different lengths of specimens having the same cross-section were tested, where strain-rate effects augment statistical effects [19], but the influence of size on strength does appear to be stronger here [23–25]. In any case, strain-rate effects should not be neglected for those brittle materials that are most susceptible to fatigue during loading. While carbonaceous materials are not very sensitive to such fatigue [26–30], the large-grained graphites most often studied from this class of materials have usually suffered from an inadequate ratio of specimen-to-grain size [22], and Weibull predictions are known to improve as this ratio increases [11–13]. Therefore, it is of interest to examine the size–strength relationship for a carbonaceous material of small grain size that is relatively insensitive to static fatigue, and glassy carbon seems to be an excellent material for this purpose [21, 28].

2. Experimental details

The plate of commercial glassy carbon* from which all specimens were taken was 125 mil† thick

*GC-1800, Beckwith Carbon Corp, Van Nuys, California, USA.
† 1 mil $\equiv 2.540 \times 10^{-5}$ m.

and had a bulk density of $1.39\,g\,cm^{-3}$. The apparent X-ray crystallite size of this material was less than 20 Å [31]. When thin strips cut from the surface of this material were polished to a mirror finish and viewed in an optical microscope under the proper angle of incident light, a great many spherical pores with diameters as large as 40 μm were observed. These observable pores become much more scarce at depths greater than 8 mil into the material, however, as previously reported [32]. Therefore, a 10 mil thickness was removed from all outer surfaces of the glassy carbon plate in order to leave the less porous bulk material; this is justified because it is possible to produce glassy carbon in the laboratory that does not have such a porous surface layer [33]. Also, the removal of surface material eliminates a residual compressive stress in that layer [28, 32], which could obscure size effects. Such a compressive surface layer, similar to that in tempered glass, is to be expected [34] when cross-linking begins at the surface during heat-treatment of the resin precursor used in producing glassy carbon [35], with the interior of the shrinking material taking longer to solidify.

In order to minimize any interior residual stress gradient [36], slices of various thicknesses were cut in such a way as to be centred about the mid-thickness plane of the plate. These thin slices, which were 4 mil thicker than the desired thicknesses of the final specimens (3, 6 and 12 mil), were sealed between glass slides with wax and then were cut into strips of the desired width (20, 40 or 80 mil) with a mechanically controlled diamond sectioning wheel. Finally, these strips were attached to an arbor and sanded down uniformly by 2 mil on each side to obtain the desired thickness, while at the same time removing the small edge chips ($<20\,\mu$m) that often resulted during cutting of the brittle glassy carbon. The final polishing compound was 3 μm diamond paste, which produced test specimens with mirror-like faces; the sides of the specimens were usually left as cut, with the diamond grit of the cutting wheel being less than 60 μm.

The finished specimens were examined under a microscope to ensure that they were free from noticeable chips or scratches, and the surface that appeared most perfect was selected to be the tension face in the three-point bend tests that were conducted. To ensure uniformity before testing, the width of each specimen was measured in a toolmaker's microscope to an accuracy of ± 0.04 mil at three points, which corresponded roughly to the load points during subsequent testing, and the thickness was measured at about the same points to an accuracy of ± 0.05 mil with a sharp-pointed micrometer. Then, after testing, dimensions of each fragment were measured adjacent to the fracture and averaged to obtain values for the actual failed section. Specimens were tested on a variable-span three-point bend fixture, having razor blades as the outer knife-edges and a sharp-pointed anvil suspended on a thin reed as the centre knife-edge; this fixture had been carefully designed for performing similar tests on pyrocarbon of the type used to coat nuclear fuel particles [37–39]. Specimens were loaded with the use of a table-model test machine at a cross-head speed of $0.01\,in.\,min^{-1}$*, and the load and deflection were simultaneously recorded. Stress-strain curves for the thinnest specimens tested became non-linear at high stresses because of large deflection effects and frictional effects at the outer knife-edges [40]. These effects were accounted for in calculating all failure stresses [39], but the resulting corrections were significant only for the 3 mil specimens, where calculated failure stresses exceeded those obtained from simple beam theory by as much as 10% for the strongest specimen tested.

3. Results and discussion

3.1. Size effect on strength

The first series of three-point bend tests conducted to determine the size effect on the strength of glassy carbon was for sets of 40 mil wide specimens having thickness of 3, 6 and 12 mil. In each case, 24 specimens were tested to failure over a span width of 0.2 in., with the specimen length being 0.4 in. Strength distributions from these tests are shown in Fig. 1, where the $n = 24$ strength values ordered from $r = 1$ to $r = n$ in decreasing magnitude have been plotted against a probability of $P = r/(n + 1)$ that an additional specimen would have for surviving each of these stresses [41]. The cumulative distribution curves for the three different specimen sizes all have essentially the same shape, as demonstrated by the near-constant value of the Weibull modulus m in the keyed upper legend of Fig. 1; this suggests that the mode of

*$1\,in.\,min^{-1} \equiv 4.233 \times 10^{-2}\,cm\,sec^{-1}$.

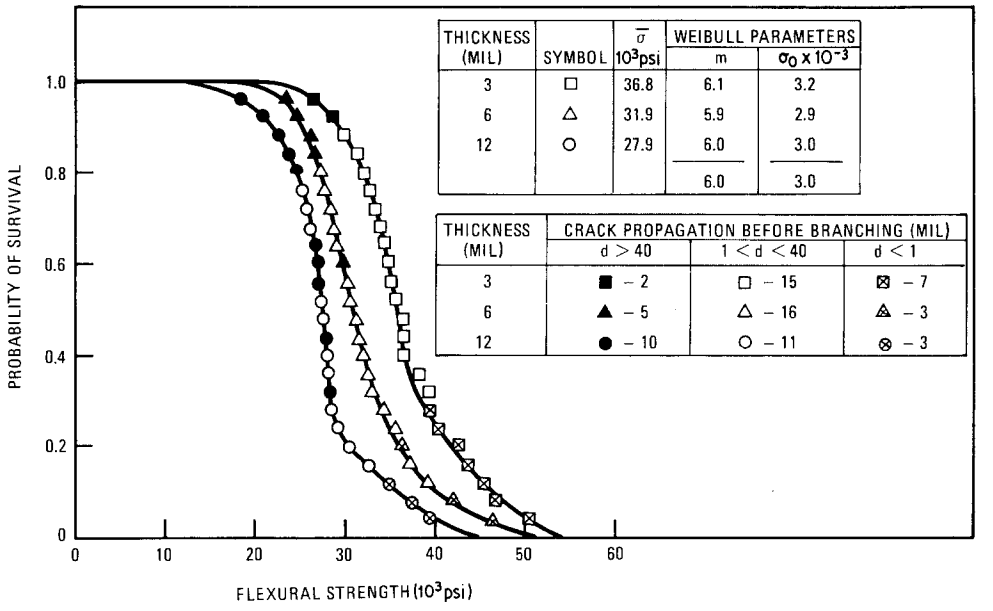

Figure 1 Strength distributions for three sizes of glassy carbon specimens.

failure is the same for all specimens. However, the strength distributions are progressively shifted to lower values as specimens become larger, with the mean strength dropping from 37 to 32 to 28 × 10^3 psi* as the specimen thickness goes from 3 to 6 to 12 mil. These differences in strength are significant at the 99% confidence level for the data in question [42], and there definitely appears to be a size effect in the direction predicted by Weibull theory. In agreement with theory, standard deviations of the strength distributions also decreased with increasing specimen size in roughly the same proportions as did mean strengths, going from 6.8 to 6.1 to 5.4 × 10^3 psi.

Additional support for the fact that thinner specimens fail at higher stresses than thicker ones can be gained from a comparison of their fracture modes, which can be related to the stress at failure. Selected fracture modes are illustrated in Fig. 2 for specimens having a common thickness (6 mil), where fractures are shown from top to bottom in order of increasing stress. In general, a crack initiates at some point along the width of a specimen and runs straight across the tensile face in both directions until one end of the crack branches to form a pie-shaped wedge, and it is observed that the total length, d, of the crack path before branching decreases as the stress increases. At the highest stress (d), the crack initiates at the edge of the specimen and runs a very short distance before branching, producing essentially a full-width wedge. As the fracture stress becomes progressively smaller for weaker and weaker specimens (c to b), the total crack path before branching lengthens, and the resulting wedges become smaller and smaller. Finally, the crack runs completely through the width of the specimen without branching at a still lower stress (a), and a clean break is produced. The origin of failure in weaker specimens (a and b) is generally located well away from the edge of the specimen, as will be discussed more fully in a subsequent section. For orientation purposes, the positions of the four specimens of Fig. 2 within the middle strength distribution of Fig. 1 are located by beginning at the top of the curve and marking points 1, 9, 21 and 24.

If the downward shift of the strength distributions of Fig. 1 with increasing specimen size is a real effect, rather than some unrecognized experimental or calculational error in determining flexural strengths [43–45], then the number of clean breaks should increase with increasing specimen size and the number of near-full wedges should decrease, because of the changing pattern of fracture mode with stress (Fig. 2). This is exactly what is found in the lower keyed legend of Fig. 1. The number of clean breaks increases

*10^3 psi ≡ 6.895 N mm^{-2}.

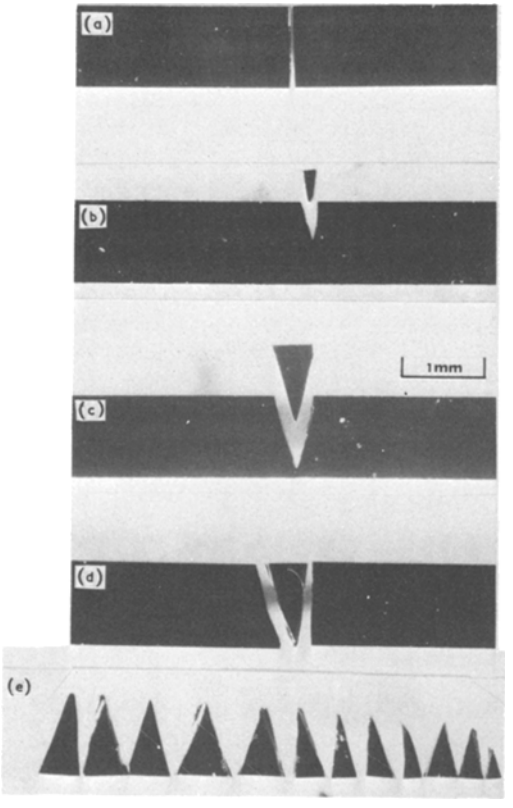

Figure 2 Selected failure modes in 40 mil wide strips of glassy carbon, looking down on tensile faces of specimens and showing (a) clean break at lowest stress (23.4×10^3 psi), (b) small wedge at moderate stress (29.0×10^3 psi), (c) large wedge at higher stress (37.2×10^3 psi), (d) full wedge at highest stress (46.3×10^3 psi), and (e) remaining collection of wedges from 6 mil thick specimens.

from two to five to ten as specimen strengths decrease with increasing size, whereas the number of near-full wedges drops from seven for the thinnest specimens to three for each of the thicker ones. A more quantitative argument along these lines will be presented after all strength measurements have been discussed, but for the moment it will be mentioned only that the changing pattern of failure mode with specimen size is in keeping with a strength decrease for increasing size.

3.2. Differentiation between various Weibull flaw distributions

Relative magnitudes of the experimental strength shifts with specimen size are compared in Table I to Weibull predictions based on three types of flaw distributions: (1) volume, (2) surface area, and (3) area of as-cut edges. The expressions given in the footnote of Table I for the strength ratios of two different sizes of specimens tested in three-point bending were obtained by setting $S_1 = S_2$, where the probability of survival S_i had been obtained by performing the integration

$$S_i = \exp\left\{-\int_\alpha [\sigma(\alpha)/\sigma_0]^m \, d\alpha\right\} \qquad (1)$$

over the appropriate distribution of tensile stress $\sigma(\alpha)$ [46], with the spatial α integration being conducted, in turn, over the specimen volume, surface area, and cut-edge area. The Weibull parameters for volume flaws in glassy carbon are

TABLE I Weibull predictions versus experimental results for 40 mil wide specimens

Strength ratios	Theory for flaws over the:			Experimental results §
	volume*	surface†	cut edge‡	
σ (3 mil)/σ (6 mil)	1.12	1.00	1.12	1.15
σ (6 mil)/σ (12 mil)	1.12	1.00	1.12	1.14
σ (3 mil)/σ (12 mil)	1.26	1.01	1.26	1.32

* $\dfrac{\sigma_1}{\sigma_2} = \left[\dfrac{s_2 w_2 t_2}{s_1 w_1 t_1}\right]^{1/m}$

† $\dfrac{\sigma_1}{\sigma_2} = \left[\dfrac{s_2\,[t_2 + w_2(m+1)]}{s_1\,[t_1 + w_1(m+1)]}\right]^{1/m}$

‡ $\dfrac{\sigma_1}{\sigma_2} = \left[\dfrac{s_2 t_2}{s_1 t_1}\right]^{1/m}$

where s is the span length for three-point bending (0.2 in.), t and w are the thickness and width of the specimen, $m = 6.0$ is the Weibull modulus for glassy carbon, and § is the ratios of standard deviations, which follow closely those of mean strengths, going from 1.11 to 1.13 to 1.26.

TABLE II Weibull predictions versus experimental results for different width specimens

Strength ratios*	Theory for flaws over:		Experimental results
	volume	cut edge	
$\sigma(3,80,75)/\sigma(12,20,75)$	1.00	1.26	0.93
$\sigma(3,80,75)/\sigma(3,40,200)$	1.05	1.18	1.04
$\sigma(3,80,75)/\sigma(6,40,200)$	1.18	1.32	1.20
$\sigma(3,80,75)/\sigma(12,40,200)$	1.32	1.48	1.37
$\sigma(12,20,75)/\sigma(3,40,200)$	1.05	0.94	1.11
$\sigma(12,20,75)/\sigma(6,40,200)$	1.18	1.05	1.28
$\sigma(12,20,75)/\sigma(12,20,200)$	1.32	1.18	1.47

*$\sigma(t, w, s)$ is the mean three-point bend strength of a specimen of thickness t and width w that is tested over a span length s, where all dimensions are in mil.

assumed to be defined by the values $m = 6$ and $\sigma_0 = 3.0 \times 10^3$ psi in.$^{3/m}$*, which were determined by averaging the closely grouped values (Fig. 1) obtained from a maximum likelihood estimate [47] for each of the three specimen sizes tested.

Agreement with experimental results is excellent for the predictions of Table I based on either a uniform distribution of flaws throughout the volume or over the surface of the cut edges of specimens, these being identical for specimens of the same width, but agreement is poor for the case where flaws are distributed over the entire surface area. In the latter case, results are dominated by the much larger surface area common to the highly polished faces of all specimens, which were thin in relation to their width, and no significant size effect is predicted. In order to separate the size effects of volume and edge flaws, additional specimens of different widths were tested. In particular, 20 mil wide specimens with a 12 mil thickness and 80 mil wide specimens with a 3 mil thickness were tested in three-point bending over a span width of 75 mil.

There should be no difference in mean strengths of these two specimens if volume flaws are controlling failure, whereas the wider 3 mil specimens should be about 26% stronger if failure is controlled by edge flaws resulting from cutting of the specimen strips. Instead, the 3 mil specimens were actually slightly weaker, based on about a dozen tests of each type only, indicating that a volume distribution of flaws is best satisfied for the glassy carbon in question. This conclusion is supported by a comparison of all combinations of the results from the two new tests with previous data for 40 mil wide specimens (Table II). Thus, intrinsic interior flaws in this glassy carbon must be more severe than edge flaws, in general, and failure will initiate at cut edges in only the very strongest specimens where interior flaws happen to be sufficiently minimized to allow edge flaws to come into play. This conclusion is confirmed by studying failure surfaces to determine origins of failure, as will be discussed in Section 3.

3.3. Strength comparisons based on a volume distribution of flaws

The appropriate probability of survival for a specimen having flaws throughout its volume and being subjected to a maximum tensile stress of σ_{max} in three-point bending can now be obtained from Equation 1 as

$$S = \exp\left[-\frac{V}{2(m+1)^2}\left(\frac{\sigma_{max}}{\sigma_0}\right)^m\right], \qquad (2)$$

where V is the volume of that portion of the specimen located between the outer knife-edges. For any volume V, this equation can be used to estimate S-σ_{max} curves of the type determined experimentally in Fig. 1. The mean value of the strength distribution from Equation 2 is given by [17]

$$\bar{\sigma} = \int_0^\infty (-dS/d\sigma_{max})\,\sigma_{max}\,d\sigma_{max} \qquad (3)$$

$$= [2(m+1)^2/V]^{1/m}\sigma_0\Gamma(1+1/m),$$

*The location parameter σ_0 is often written in terms of stress units only, with the volume obtained on integration then being regarded as a dimensionless quantity that expresses the number of unit volumes involved. This eliminates an awkward unit, but it could lead to confusion when σ_0 is rewritten in another system of units, e.g. $\sigma_0 = 3.29\,\mathrm{MN\,m^{-3/2}}$. Notice that σ_0 does not appear in the strength ratios of Table I and that the derived m value does not depend on any assumption regarding the type of flaw distribution.

TABLE III Three-point bend data for glassy carbon

Test no.	Dimensions (mil)			No. spec.	Mean strength (10^3 psi)		
	Thickness	Width	Span		Expt.	Calc.*	% diff.
1	3	40	200	24	36.8	35.0	4.9
2	6	40	200	24	31.9	31.6	0.9
3	12	40	200	24	27.9	27.8	0.3
4	3	80	75	10	38.2	36.1	5.5
5	12	20	75	12	40.9	36.9	9.8

* $\bar{\sigma} = \left[\frac{2(m+1)^2}{V}\right]^{1/m} \sigma_0 \Gamma(1 + 1/m)$,

where $m = 6.0$ and $\sigma_0 = 3.0 \times 10^3$ psi in.$^{3/m}$.

where $\Gamma(x)$ is the gamma function of argument $x = 1 + 1/m$.

Mean strengths for the five different sizes of glassy carbon specimens tested are given in Table III, and these experimental results are compared to calculated values obtained from Equation 3 using the best single set of Weibull parameters determined from the first three tests, which were considered to be the most reliable. Differences between experiment and theory are less than 5% for the three different thicknesses of 40 mil wide specimens, where 24 specimens of each type were tested, and differences are less than 10% for the specimens of other widths in which only about one-half as much testing was done. This agreement is regarded to be entirely satisfactory, considering the uncertainties involved, and lends strong support for a Weibull size effect based on the volume of glassy carbon under test.

The volume dependence of the mean flexural strength of glassy carbon predicted by Equation 3 is shown in the upper curve of Fig. 3, and experimental values for the three specimen sizes that were used to determine the Weibull parameters are also shown. The lower curve of Fig. 3 shows the expected volume dependence of the mean tensile strength of glassy carbon, which is given by

$$\bar{\sigma} = V^{-1/m} \sigma_0 \Gamma(1 + 1/m). \quad (4)$$

From another source [48], the measured tensile strength is shown for a 1 cm gauge length of a 25 μm glassy carbon fibre having the same elastic modulus ($E = 4 \times 10^6$ psi) as the material investigated, and this too agrees well with theory. Yet another strength measurement within the volume range of Fig. 3 that agrees well with theory is the three-point bend strength of 31.9×10^3 psi reported [49] for a test volume of 4×10^{-5} in.^{3}. It can also be inferred from the literature that the two curves of Fig. 3 project very nicely to larger volumes of glassy carbon. The measured flexural strength for a volume of 0.01 in.^{3} is about 12×10^3 psi [50], whereas Equation 3 predicts

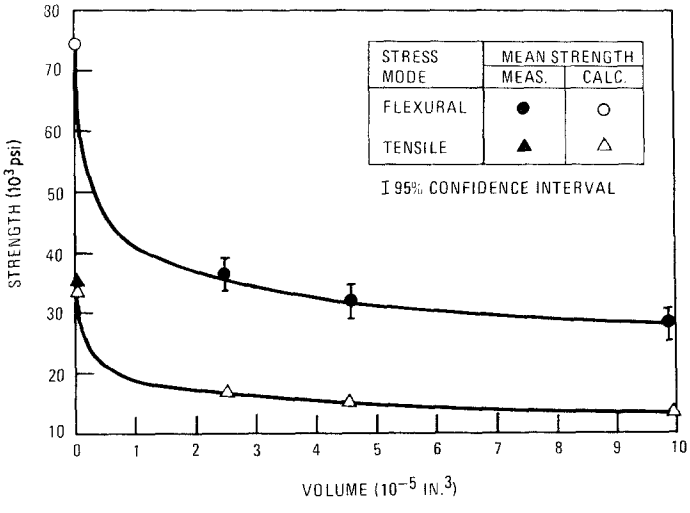

Figure 3 Size effect on mean strength of glassy carbon.

12.9×10^3 psi. Likewise, the measured tensile strength for a volume of 0.006 in.^{3} is about 6×10^3 psi [51], and Equation 4 gives 6.5×10^3 psi. Therefore, strengths reported for all commercial glassy carbons seem to correlate well with Weibull theory when the common set of parameters determined in this study is used.

3.4. Implications of crack bifurcation

The most common type of fracture for the 40 mil wide specimens in the first series of tests involved running cracks that branched on one end only (Fig. 2). With the exception of those cases in which near full-width wedges had been produced by the branching of cracks originating at a specimen edge (Fig. 2d), it was not possible to pinpoint the origin of failure within the tail of the Y-shaped cracks from an examination of specimen tensile surfaces. Instead, a detailed study of that part of the thin fractured cross-section that fits together smoothly was required to locate the likely origin of failure within the smooth "mirror region" produced by the straight running crack before it first began to branch (Fig. 4). The second series of tests on different width specimens was undertaken before such likely origins had been determined in order to assess the relative importance of volume and edge flaws, as there was concern at that time that failures might be originating from edge flaws produced in cutting the specimen strips. However, strength ratios of the different width specimens indicated that edge flaws were not primarily responsible for failure (Table II), and this conclusion was supported by examining fracture surfaces to locate internal flaws (Fig. 4). Also the testing of wider specimens allowed increased opportunity for branching to develop on both ends of cracks emanating from interior flaws, as illustrated in Fig. 5, and a simple examination of specimen tensile faces served to locate failure origins at the centres of single-path segments when this occurred. A view of the fracture cross-section for a failure of this type is shown in Fig. 6, where the source of failure S is now located along the vertical centreline of the mirror region M.

In addition to verifying a volume distribution for the Weibull flaws that control strengths of glassy carbon, a study of crack bifurcation also provides quantitative support for the Weibull strength shifts shown in Fig. 1. When strength values σ_i of Fig. 1 for specimens of all thicknesses are plotted against the distance r_i from the origin

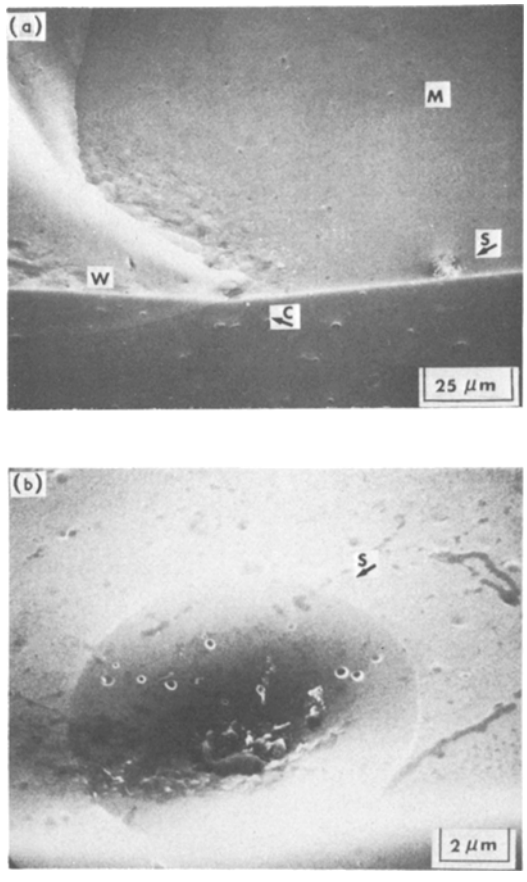

Figure 4 SEM fractographs of (a) the mirror region M surrounding the likely source of failure S, which is well away from the nearest specimen cut edge to the right, and (b) the inherent spherical pore where failure probably initiated. Notice that the crack has formed a Y-type branch at C, producing a wedge W that did not completely separate as in Fig. 2. The total crack length d before branching, which was used in Fig. 1 as the basis for a preliminary classification of failure that did not require the location of S, would be measured here from C to the specimen edge toward which the apex of W points, since no other branch point is encountered along that distance.

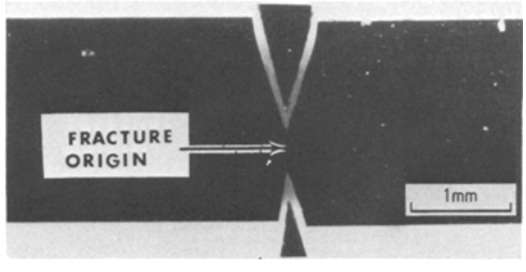

Figure 5 Double-wedge fracture from an interior flaw in an 80 mil wide strip of glassy carbon.

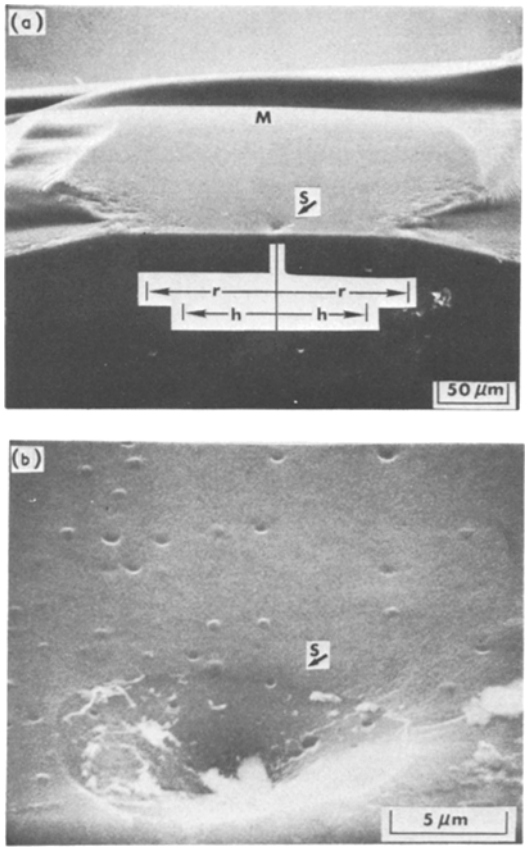

Figure 6 SEM fractographs of (a) mirror region and (b) origin of failure for a double-wedge fracture. Noting the flaw half-length to be $c = 7.5\,\mu m$ for this specimen that failed at 29.2×10^3 psi, the energy required to produce each new unit area of fracture surface is calculated from a modified Griffith relationship for circular flaws to be $\gamma = 0.04$ in.$^{-1} = 7.0$ J m^{-2}; this is roughly the average value obtained for the glassy carbon in question, as is the r/c ratio of 13.5 found for this specimen. Thus, the modified Griffith equation for this case reduces to give the observed bifurcation relationship of $\sigma r^{1/2} = 1.9 \times 10^3$ psi in.$^{1/2}$.

of fracture to the point of bifurcation (Fig. 6), measured along a line of constant tension in the fracture surface, the points scatter about a straight line of slope $-\frac{1}{2}$ on a log–log plot [50]. This implies that

$$\sigma r^{1/2} = \text{constant}, \tag{5}$$

a relationship initially derived for glass [52–55] and subsequently verified for a wide variety of brittle materials [56–61]. The value of this constant, K, for gross branching of glassy carbon is 1.9×10^3 psi in.$^{1/2}$ (2.09 MN m$^{-3/2}$); this is about 20% larger than the value previously reported [50], but that value was obtained by measuring r from the failure origin to the closer "hackle boundary", h, where microscopic branching could first be detected by surface roughening (Fig. 6).

Data points for glassy carbon specimens of a particular size are concentrated within different regions when σ_i is plotted against r_i, as found for ordinary glass [62], but all sizes define essentially the same value of K. Therefore, an average strength for the n specimens of each size can also be calculated by the use of Equation 5 as

$$\bar{\sigma} = \frac{K}{n} \sum_{i=1}^{n} r_i^{-1/2}, \tag{6}$$

and these values are in roughly the same proportions for the different size specimens as the directly measured strengths (Table I). Thus, given the validity of Equation 5, which is equivalent to the Griffith relationship [63] since r is found to be a constant multiple of the flaw size responsible for brittle failure initiation in a given material [59, 64], there is independent support for the measured downward shift of strength with increasing specimen size.

Most studies on crack branching have made use of thick specimens in order to observe the full mirror, mist, and hackle patterns that are produced on the fractured cross-section [50, 55], but wedge-shaped fragments such as those shown in Figs. 2 and 5 are not usually produced in such cases. The sides of these triangular wedges were usually straight, and the wedge shape did not change as its size varied with stress (Fig. 2e). The average branching angles were inclined at about $\pm 15^\circ$ with respect to the initial plane of the crack, producing wedges with an apex angle of about 30°. A brief outline of the physical basis proposed for crack bifurcation will be useful in discussing this branching symmetry. The propagation speed of a running crack in a brittle material increases with increasing path length until it reaches a limiting value, which is about 60% of the speed of a shear wave in that material [50]. The stress distribution about the tip of the running crack is sufficiently distorted [65] when this occurs to give maximum tangential stresses at angle of $\pm\theta$ with respect to the initial direction of propagation [66]. Consequently, the observed symmetric Y-type branching is expected from theory.

There is a large discrepancy as to what the branching angle should be, however, for theory

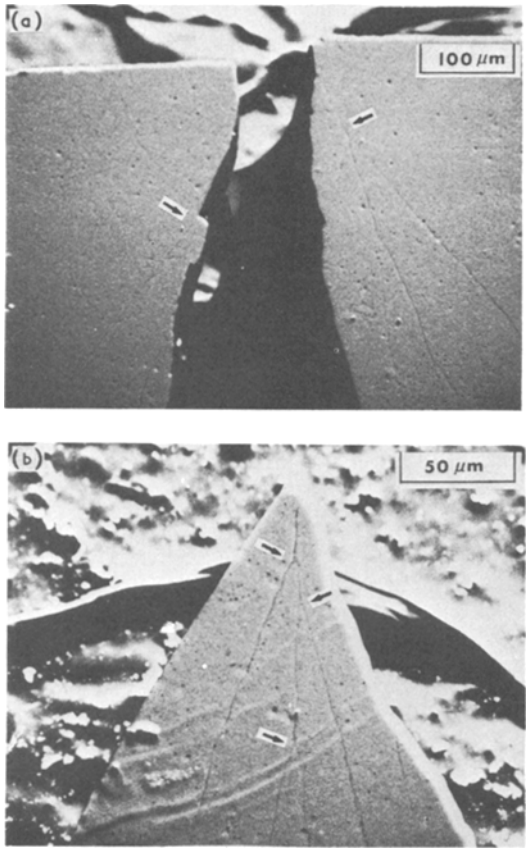

Figure 7 SEM micrographs of secondary cracks on tensile faces of (a) the two main segments of a failed specimen and (b) the wedge-shaped fragment formed by primary crack bifurcation.

predicts maximum stresses at $\pm 60^\circ$ for high crack speeds [66] and the average measured valve from separated wedges is only ± 15, with values ranging from $\pm 11^\circ$ to $\pm 23^\circ$. Branching cracks with wider angles than these were occasionally observed on the tensile face of the two main sections of reassembled specimens (Fig. 7a), where these cracks did not extend through to the compression face, but the wider angles were never more than $\pm 30^\circ$. Also, wedges were often bisected part way through by the undeviated primary crack, and this partial crack itself sometimes branched more narrowly further on along its path (Fig. 7b). Therefore, branching angles seem to narrow with distance of travel, and better agreement might be expected if angles could be measured where microscopic cracking first begins [67], which is also the region where theory has the most validity [68]. However, the theory itself is still unsettled [68, 69], as there is disagreement as to whether branching is more critically dependent on crack velocity [66], the attainment of sufficient total energy to form and propagate new crack surfaces [50], or the reaching of a critical stress intensity factor at the crack tip [56, 70].

4. Conclusions

The more important results of this study on commercial glassy carbon are as follows:

(1) The strength dependence on size is well represented by Weibull theory when flaws are assumed to be distributed throughout the volume of the material.

(2) The Weibull parameters are given by $m = 6.0$ and $\sigma_0 = 3.0 \times 10^3$ psi in.$^{3/m}$.

(3) Mean strengths in three-point bending and in tension, respectively, are well approximated for any volume V(in.^{3}) by $5.98V^{-1/6} \times 10^3$ psi and by $2.78V^{-1/6} \times 10^3$ psi.

(4) If σ is the failure stress for a specimen and r is the distance from the origin of failure to the point where the crack branches macroscopically, then $\sigma r^{1/2} =$ constant, with 1.9×10^3 psi in.$^{1/2}$ being the value of the constant.

(5) The observed values of r can be used in conjunction with the bifurcation relation above to compute mean strengths for the different specimen sizes that were tested; these strengths are in general agreement with the directly measured ones, providing additional support for the validity of the Weibull volume relationship.

(6) Shapes of the triangular wedges separated from specimens as a result of crack branching did not change as their sizes varied with failure stress, and the branching angles were found to be tightly grouped around $\pm 15^\circ$.

(7) Origins of failure were usually internal spherical pores with diameters in the range of 5 to 40 μm for this glassy carbon, and measured strengths for specimens having these various flaw sizes agreed well with Griffith theory if the fracture surface energy was taken to be 0.04 lb in.$^{-1}$ (7.0 J m^{-2}), where the usual sharp-crack form of the Griffith equation was multiplied by a geometrical factor of $\pi/2$ to account for the presence of interior circular flaws [71]. The mean size of critical flaws for the different sets of specimens tested increased with test volume, going from approximately 10 μm for 3 mil thick specimens to 20 μm for 12 mil thick specimens. If the mean critical pore size of a glossy carbon could be

reduced to the rather uniformly distributed 1 μm background pores observed here, then the flexural strength should increase to over 100×10^3 psi if no other flaw types were present.

Acknowledgements

The authors wish to acknowledge the help of F. J. Gagnon in the careful preparation of the test specimens and also that of D. R. Wall for providing the SEM micrographs of failed specimens.

References

1. R. E. BULLOCK, *J. Comp. Mater.* 8 (1974) 200.
2. D. R. PLATTS and H. P. KIRCHNER, *J. Materials* **6** (1971) 48.
3. Ö. VARDAR and I. FINNIE, *Int. J. Fract.* **11** (1975) 495.
4. M. C. SHAW, P. M. BRAIDEN and G. J. DESALVO, *Trans. ASME, J. Eng. Ind.* **97** (1975) 77.
5. D. G. S. DAVIES, *Proc. Brit. Ceram. Soc.* **22** (1973) 429.
6. M. KNIGHT and H. T. HAHN, *J. Comp. Mater.* 9 (1975) 77.
7. G. K. BANSAL, W. H. DUCKWORTH and D. E. NIESZ, *J. Amer. Ceram. Soc.* **59** (1976) 472.
8. P. MARSHALL and E. K. PRIDDLE, *Carbon* **11** (1973) 627.
9. R. J. PRICE and H. R. W. COBB, "Application of Weibull Statistical Theory to the Strength of Reactor Graphite", in Proceedings of the Conference on Continuum Aspects of Graphite Design, Gatlinburg, Tenn., 9–12 November (1970) (USAEC Document No. CONF-701105) pp. 547–67.
10. R. J. PRICE, "Statistical Study of the Strength of Near-Isotropic Graphite", in Extended Abstracts for the 12th Biennial Conference on Carbon, the American Carbon Society, Pittsburgh, Pa., 28 July to 1 August (1975) pp. 145–6.
11. I. B. MASON, "The Strength of Commercial Graphite", in Proceedings of the Fifth Conference on Carbon, Vol. 2 (Pergamon Press, New York, 1960) pp. 597–610.
12. R. KREFELD and V. LUNGAGNANI, "Application of Weibull's Theory to the Strength of Irradiated Isotropic Graphite", in Summary of Papers for the 9th Biennial Conference on Carbon, the American Carbon Society, Boston, Mass., 16–20 June (1969) p. 106.
13. F. LANZA and H. BURG, "Investigation of the Volume Effect on Mechanical Properties of Various Industrial Graphites", in Extended Abstracts for the 11th Biennial Conference on Carbon, the American Carbon Society, Gatlinburg, Tenn., 4–8 June (1973) pp. 223–4.
14. J. AMESZ, J. DONEA and F. LANZA, "Comparison of Mechanical Properties in Bending and Tensile Tests for Industrial Graphites", *ibid.* pp. 221–3.
15. R. KREFELD, G. LINKENHEIL and J. MEELDIJK, "The Effect on High Temperature Fast Neutron Irradiation on the Distribution Functions of Strength of Some Nuclear Graphites", in Summary of Papers for the 10th Biennial Conference on Carbon, the American Carbon Society, Bethlehem, Pa., 27 June-2 July (1971) pp. 179–80.
16. G. K. BANSAL, W. DUCKWORTH and D. E. NIESZ, *Amer. Ceram. Soc. Bull.* **55** (1976) 289.
17. D. LEWIS and S. M. OYLER, *J. Amer. Ceram. Soc.* **59** (1976) 507.
18. J. E. BROCKLEHURST and M. I. DARBY, *Mat. Sci. Eng.* **16** (1974) 91.
19. D. P. H. HASSELMAN, G. B. KENNEY and K. R. MCKINNEY, *J. Amer. Ceram. Soc.* **58** (1975) 452.
20. J. E. RITTER, Jun. and K. JAKUS, *ibid.* **60** (1977) 192.
21. W. P. MINNEAR and R. C. BRADT, *ibid.* 58 (1975) 345.
22. A. W. THOMPSON, *Scripta Met.* 8 (1974) 145.
23. D. LEWIS, *Amer. Ceram. Soc. Bull.* **54** (1975) 310.
24. J. B. BARR, S. CHWASTIAK and R. DIDCHENKO, "High Strength Carbon Fibers from Mesophase Pitch", in Extended Abstracts for the 13th Biennial Conference on Carbon, the American Carbon Society, Irvine, Ca., 18–22 July (1977) pp. 96–7.
25. R. BACON and W. A. SCHALAMON, in "High Temperature Resistant Fibers from Organic Polymers", edited by J. Preston (Interscience, New York, 1969) pp. 285–91.
26. B. J. S. WILKINS, *J. Amer. Ceram. Soc.* **54** (1971) 593.
27. P. H. HODKINSON and J. S. NADEAU, *J. Mater. Sci.* **10** (1975) 846.
28. J. S. NADEAU, *J. Amer. Ceram. Soc.* **57** (1974) 303.
29. F. J. SCHOEN, *Carbon* **11** (1973) 413.
30. S. J. BAKER and W. BONFIELD, *J. Mater. Sci.* **10** (1975) 1015.
31. J. L. KAAE, "The Effect of Microporosity on Graphitizability of Glassy Carbon", pp. 414–15 in [24].
32. J. S. NADEAU, *J. Amer. Ceram. Soc.* **56** (1973) 467.
33. E. FITZER, W. SCHAEFER and S. YAMADA, *Carbon* **7** (1969) 643.
34. F. M. ERNSBERGER, *Amer. Ceram. Soc. Bull.* **54** (1975) 533.
35. E. FITZER and W. SCHAEFER, *Carbon* 8 (1970) 353.
36. F. M. ERNSBERGER, *Amer. Ceram. Soc. Bull.* **52** (1973) 240.
37. J. C. BOKROS and R. J. PRICE, *Carbon* 3 (1966) 503.
38. J. L. KAAE, *ibid* **10** (1972) 691.
39. *Idem, J. Nucl. Mater.* **46** (1973) 121.
40. J. L. KAAE and T. D. GULDEN, *J. Amer. Ceram. Soc.* **54** (1971) 605.
41. W. WEIBULL, *Ingenioersvetenskapsakad. Handl.* **151** (1939) 45 pp.
42. W. B. HALL, L. R. JOHNSON and M. W. PARKER, *Amer. Ceram. Soc. Bull.* **55** (1976) 1004.
43. W. H. DUCKWORTH, *J. Amer. Ceram. Soc.* **34** (1951) 1.

44. R. G. HOAGLAND, C. W. MARSHALL and W. H. DUCKWORTH, *ibid* **59** (1976) 189.
45. B. W. ROSEN and N. F. DOW, in "Fracture", Vol. VII, edited by H. Liebowitz (Academic Press, New York, 1972) pp. 611–74.
46. N. A. WEIL and I. M. DANIEL, *J. Amer. Ceram. Soc.* **47** (1964) 286.
47. J. W. HEAVENS and P. N. MURGATROYD, *ibid.* **53** (1970) 503.
48. K. KAWAMURA and G. M. JENKINS, *J. Mater. Sci.* **7** (1972) 1099.
49. J. L. KAAE, *J. Biomed. Mater. Res.* **6** (1972) 279.
50. J. J. MECHOLSKY, R. W. RICE and S. W. FREIMAN, *J. Amer. Ceram. Soc.* **57** (1974) 440.
51. W. V. KOTLENSKY and H. E. MARTENS, "Tensile Behavior of Glassy Carbon at Temperatures up to 2900° C"; paper V-2 in Symposium on Carbon, Carbon Society of Japan, Tokyo, 20–23 July, (1964).
52. W. C. LEVENGOOD, *J. Appl. Phys.* **29** (1958) 820.
53. E. B. SHAND, *J. Amer. Ceram. Soc.* **42** (1959) 474.
54. M. J. KERPER and T. G. SCUDERI, *Amer. Ceram. Soc. Bull.* **43** (1964) 622.
55. J. W. JOHNSON and D. G. HOLLOWAY, *Phil. Mag.* **14** (1966) 731.
56. J. CONGLETON and N. J. PETCH, *ibid* **16** (1967) 749.
57. H. P. KIRCHNER and R. M. GRUVER, *ibid* **27** (1973) 1433.
58. H. P. KIRCHNER, R. M. GRUVER and W. A. SOTTER, *J. Amer. Ceram. Soc.* **58** (1975) 188.
59. J. J. MECHOLSKY, S. W. FREIMAN and R. W. RICE, *J. Mater. Sci.* **11** (1976) 1310.
60. G. K. BANSAL and W. H. DUCKWORTH, *J. Amer. Ceram. Soc.* **60** (1977) 304.
61. G. K. BANSAL, *Phil. Mag.* **35** (1977) 935.
62. M. J. KERPER and T. G. SCUDERI, *Amer. Ceram. Soc. Bull.* **45** (1966) 1065.
63. A. A. GRIFFITH, *Phil. Trans. Roy. Soc. London* **221A** (1920) 163.
64. D. A. KROHN and D. P. H. HASSELMAN, *J. Amer. Ceram. Soc.* **54** (1971) 411.
65. B. COTTERELL, *Int. J. Fract.* **1** (1965) 96.
66. E. H. YOFFE, *Phil. Mag.* **42** (1951) 739.
67. J. W. JOHNSON and D. G. HOLLOWAY, *ibid* **17** (1968) 899.
68. J. E. FIELD, *Contemp. Phys.* **12** (1971) 1.
69. L. R. F. ROSE, *Int. J. Fract.* **12** (1976) 799.
70. K. R. MCKINNEY, *J. Amer. Ceram. Soc.* **56** (1973) 225.
71. D. C. CRANMER, R. E. TRESSLER and R. C. BRADT, *ibid.* **60** (1977) 230.

Received 20 June and accepted 6 September 1978.